



# HOKKAIDO UNIVERSITY

Title	Dielectric properties of Al-Si composite oxide films formed on electropolished and DC-etched aluminum by electrophoretic sol-gel coating and anodizing
Author(s)	Sunada, M.; Takahashi, H.; Kikuchi, T. et al.
Citation	Journal of Solid State Electrochemistry, 11(10), 1375-1384 <a href="https://doi.org/10.1007/s10008-007-0316-2">https://doi.org/10.1007/s10008-007-0316-2</a>
Issue Date	2007-10
Doc URL	<a href="https://hdl.handle.net/2115/28635">https://hdl.handle.net/2115/28635</a>
Rights	The original publication is available at <a href="http://www.springerlink.com">www.springerlink.com</a>
Type	journal article
File Information	JSSE11-10.pdf



Dielectric Properties of Al-Si Composite Oxide Films Formed on Electropolished and  
DC-Etched Aluminum by Electrophoretic Sol-Gel Coating and Anodizing

M. Sunada<sup>a</sup>, H. Takahashi<sup>a</sup>, T. Kikuchi<sup>a</sup>, M. Sakairi<sup>a</sup>, and S. Hirai<sup>b</sup>

<sup>a</sup>Graduate School of Engineering, Hokkaido University

<sup>b</sup>Faculty of Engineering, Muroran Institute of Technology

Abstract

Highly pure aluminum specimens (99.99 %) after electropolishing and DC-etching were covered with SiO<sub>2</sub> films by electrophoretic sol-gel coating, and were anodized in neutral boric acid / borate solutions. Time-variations in cell voltage during electrophoretic sol-gel coating and in anode potential during anodizing were monitored. Structure and dielectric properties of the anodic oxide films were examined by SEM, TEM, EDX, and electrochemical impedance spectroscopy (EIS).

It was found that electrophoretic sol-gel coating forms uniform SiO<sub>2</sub> films on the

surface of both electropolished and DC-etched specimens. Anodizing of specimens after electrophoretic coating lead to the formation of anodic oxide films consisting of two layers: an inner alumina layer and an outer Al-Si composite oxide layer. The anodic oxide films formed thus had slightly higher capacitances than those formed on aluminum without any coating. Higher heating temperatures after electrophoretic deposition caused the increase in capacitance of anodic oxide films more effectively. Anodizing in a boric acid solution after SiO<sub>2</sub> coating on DC-etched foil allowed the anode potential to reach a value higher than 1,000 V, resulting in 39% higher capacitances than those on specimens without SiO<sub>2</sub> film.

#### Keywords

Aluminum, Electrolytic capacitor, Electrophoretic deposition, Sol-gel coating,

Composite oxide film

#### 1. Introduction

Aluminum electrolytic capacitors, which use aluminum anodic oxide films as a

dielectric layer, have high electric capacitance, self-repairing ability, and high voltage sustainability, and are used in many electric circuits with switching regulator, AC-DC inverter and others. Recent development in hybrid and electric vehicle strongly requires small electrolytic capacitors with high electric capacitance and high voltage sustainability. The capacitance,  $C$ , of the electrolytic capacitor can be expressed by the following equation.

$$C = \epsilon_0 \epsilon S / \delta \quad (1)$$

where  $\epsilon_0$  is the vacuum permittivity,  $\epsilon$  the relative dielectric constant of anodic oxide films,  $S$  the surface area, and  $\delta$  the film thickness. This equation indicates that  $C$  value is directly proportional to the dielectric constant of oxide films and surface area, and inversely proportional to the film thickness.

Increase in  $S$  is attained by electrochemical etching of the aluminum substrate before anodizing in electrolytic capacitor manufacturing industry. Etching with direct current (DC-etching) is used for high voltage sustainable capacitors, while alternative

current etching (AC-etching) for low voltage sustainable capacitors. Decrease in  $\delta$  can be achieved by forming anodic oxide films with low K-values<sup>1-6</sup>. The K-value is defined as the ratio of film thickness against film formation potential ( $\delta / E_a$ ). Anodic oxide films containing crystalline oxides have low K-values, since strong chemical bonds in crystalline oxides may enable higher electric fields across the oxide. Increase in  $\epsilon$ -values of anodic oxide films can be only slightly achieved by the formation of crystalline oxides, but may be achieved vigorously by incorporating metal oxides, which have high  $\epsilon$ -values<sup>7-13</sup>.

In previous studies, the authors developed a new process, which was anodizing after sol-gel dip coating of valve metal oxides<sup>14-22</sup>. It was found in the study that anodizing of Al specimens after SiO<sub>2</sub>-coating by sol-gel dip coating causes the formation of anodic oxide films including an Al-Si composite oxide layer. This film had high voltage sustainability and at most about 20% higher parallel capacitance than anodic oxide films on electropolished aluminum without any coating. However, the sol-gel dip coating was insufficient for uniform coating of SiO<sub>2</sub> films on DC-etched aluminum with micro-tunnel pits.

In the present investigation, the authors attempt to form Al-Si composite oxide films by electrophoretic sol-gel coating<sup>23 - 25)</sup> and anodizing on both electropolished and DC-etched aluminum foil to examine dielectric properties of the composite oxide film.

## 2. Experimental

### 2.1 Specimens

Highly pure aluminum foil (99.99 %) was used as specimens after electropolishing (Specimen-I) or DC-etching (Specimen-II, supplied by Nippon Chemi-Con Co.). In a preliminary experiment, both types of specimens were anodized at 5 V in  $0.5 \text{ kmol m}^{-3}\text{-H}_3\text{BO}_3 / 0.05 \text{ kmol m}^{-3}\text{-Na}_2\text{B}_4\text{O}_7$  solution to compare the parallel capacitance of anodic oxide films on Specimen-I with that on Specimen-II. It was assumed from the preliminary experiment that the surface area of specimen-II is twenty times as large as that of Specimen-I. In the present study, currents in electrophoretic sol-gel deposition and anodizing were determined so that the current density is the same on both types of specimens. The size of specimens exposed to the solutions during electrophoretic deposition and anodizing was  $4 \times 10^{-4} \text{ m}^2$  on Specimen-I and  $0.4 \times 10^{-4}$

m<sup>2</sup> on Specimen-II.

Specimen-I, which had been electropolished in a HClO<sub>4</sub> / CH<sub>3</sub>COOH solution, was dipped in ethanol and kept in a silica gel desiccator before sol-gel coating, while Specimen-II, which had been DC-etched, was dipped in ethanol and kept in a vacuum desiccator.

## 2.2 SiO<sub>2</sub> -film coating by electrophoretic sol-gel method

A sol composed of tetra-ethoxysilane (Si(OC<sub>2</sub>H<sub>5</sub>)<sub>4</sub>), NH<sub>3</sub>, distilled water and dehydrated ethanol (1 : 0.07 : 5.75 :17.6 in molar ratio) was prepared in a glove box at room temperature under N<sub>2</sub>-atmosphere. Relative humidity in the grove box was kept below 2.0 %<sup>17)</sup>. Specimen-I or -II as an anode and a platinized Pt electrode as a cathode were dipped into the sol, and constant currents of  $i_c = 0.05 - 0.2 \text{ A m}^{-2}$  were applied until cell voltage,  $V_c$ , reaches a preset value. After the electrophoretic deposition, the specimens were withdrawn from the sol at  $0.3 \text{ mm s}^{-1}$ , dried at 298 K for 300 s, and heated at  $T_h = 573, 673, \text{ and } 773 \text{ K}$  for  $t_h = 1.8 \text{ ks}$  in O<sub>2</sub> atmosphere<sup>17)</sup>. After coatings, mass gains of the specimens were measured by a microbalance. In a

part of experiments, the process of electrophoretic deposition, drying, and heating were repeated at most  $n = 2$  times.

Sol-gel dip coating was also carried out to compare the uniformity of  $\text{SiO}_2$  film coated by electrophoretic coating with that by dip coating. In the dip coating, Specimens-I, and -II were immersed into the sol for 300 s on open circuit, and then dried / heated under the same conditions as the electrophoretic coating.

### 2.3 Anodizing

The specimens coated with  $\text{SiO}_2$  film were anodized with a constant current of  $i_a = 10 \text{ A m}^{-2}$  at  $T_a = 293 \text{ K}$  in  $0.5 \text{ kmol m}^{-3}\text{-H}_3\text{BO}_3 / 0.05 \text{ kmol m}^{-2}\text{-Na}_2\text{B}_4\text{O}_7$  solution (Solution-I) and  $0.5 \text{ kmol m}^{-3}\text{-H}_3\text{BO}_3$  solution (Solution-II). Specimens without  $\text{SiO}_2$ -films were also anodized under the same conditions. The change in anode potential,  $E_a$  (vs.  $\text{Ag}/\text{AgCl}$ ), with time,  $t_a$ , during anodizing was monitored by a digital multi-meter connected to a PC system. The measurement of  $E_a$  was carried out with a three electrode system, consisting of Pt counter electrode and  $\text{Ag} / \text{AgCl}$  reference electrode as well as Al working electrode during anodizing in Solution-I, while during anodizing

in Solution-II a two electrode system, consisting of Al working electrode and Pt counter electrode, was used to estimate  $E_a$  by subtracting the solution potential drop from cell voltage. The application of the two-electrode system is because of avoidance of the current flow through reference electrode, due to the increase in anode potentials up to as high as 1,000 V during anodizing in Solution-II.

#### 2.4 Characterization

Sections of anodic oxide films formed after  $\text{SiO}_2$ -coating were examined by transmission electron microscopy (TEM, HITACHI H-700H) using an ultra thin sectioning technique, and analyzed with energy dispersed X-ray analyzer (EDX, JEOL JEM-2000ES). The surface of specimens after  $\text{SiO}_2$ -coating and anodizing was observed by scanning electron microscopy (FE-SEM, JEOL JSM-6300 F). A thin layer of platinum was coated on the specimens prior to SEM.

Electrochemical impedance spectroscopy (EIS, NF-S5720B) was performed in  $0.5 \text{ kmol m}^{-3}\text{-H}_3\text{BO}_3 / 0.05 \text{ kmol m}^{-2}\text{-Na}_2\text{B}_4\text{O}_7$  solution using sinusoidal wave of 10 mV amplitude.

Frequency range of the signal was 0.1 Hz ~ 50 kHz. Parallel capacitances of anodic oxide films,  $C_p$ , were estimated by analyzing Bode diagrams of EIS.

### 3. Results and discussion

#### 3.1 SiO<sub>2</sub> films coated by electrophoretic deposition

Figure 1 shows the time-variations in cell voltage,  $V_c$ , during electrophoretic deposition of SiO<sub>2</sub> with different current densities of  $i_c = 0.01 - 0.2 \text{ A m}^{-2}$  on a) Specimen-I and b) Specimen-II. On Specimens- I and II,  $V_c$  shows a jump at the initial stage of deposition, and then, increases linearly with coating time,  $t_c$ . With increasing  $i_c$ , the  $V_c$ -jump becomes more remarkable and the slope of  $V_c$  vs.  $t_c$  curves becomes steeper. The voltage jump at the initial stage on Specimen-II is higher than that on Specimen-I, and that the slope of  $V_c$  vs.  $t_c$  curve on Specimen-II is as high as that of specimen-I at each  $i_c$ . This suggests that the  $V_c$ -jump is due to IR-drop of sol, and the increase in  $V_c$  with  $t_a$  is due to the deposition of SiO<sub>2</sub> sol and the formation of anodic oxide films. The larger IR drop of sol on Specimen-II is considered to be due to its micro-pit structure.

Figure 2 shows the effect of heating temperature,  $T_h$ , on the  $V_c$  vs.  $t_c$  curve during the second step ( $n = 2$ ) on Specimen-I with  $i_c = 0.2 \text{ A m}^{-2}$ . In the first step,  $\text{SiO}_2$  gel was deposited with  $i_c = 0.2 \text{ A m}^{-2}$  up to  $E_c = 5 \text{ V}$ , and then heat treatment was carried out at  $T_h = 573, 673, \text{ and } 773 \text{ K}$  for  $t_h = 1.8 \text{ ks}$ . Each curve shows a jump of  $V_c$  at the initial stage of the deposition, and then a rapid decrease in  $V_c$  before reaching a steady value. After the steady  $V_c$  between 10 and 150 s,  $V_c$  increases linearly with coating time,  $t_c$ . It can be seen from Fig. 3 that higher  $T_h$ s lead to higher steady values of  $V_c$ , shorter steady  $V_c$  periods, and flatter slopes of  $V_c$  vs.  $t_c$  curves after the steady period. Higher heating temperatures is considered to cause more evaporation of organic compounds and dehydration of  $\text{SiO}_2$  gel, resulting in the formation of more anhydrous  $\text{SiO}_2$  with more micro-cracks, although the effect of heating temperature,  $T_c$ , in the first coating process on the second coating process has not been examined further.

Figure 3 is TEM images of the cross section of Specimen-I after electrophoretic deposition up to  $V_c = 10 \text{ V}$  by a) one step ( $n = 1$ , see Fig. 1-a) and b) two steps ( $n = 2$ , see Figs. 1-a. and 2). Both specimens were heated at  $T_h = 573 \text{ K}$  for  $t_h = 1.8 \text{ ks}$  after each deposition step. There are two layers on the specimen surface in both photos: an

inner dark layer with 15 nm thickness and an outer gray layer with 50 - 80 nm thicknesses. The outer layer is SiO<sub>2</sub> layer deposited from sol, and the inner layer is the oxide layer formed by anodic oxidation, which may consist of Al-Si composite oxide. The SiO<sub>2</sub> layer is thicker on the specimen coated by one step than by two steps, while the thickness of the Al-Si composite oxide layer does not depend on the repetition number, n. Judging from the inner layer thickness, one can assume that the anodic oxide layer sustains the most of cell voltage during electrophoretic deposition.

Figure 4 is TEM images of the cross sections of Specimen-II after a) dip coating (low magnification), b) dip coating (high magnification), c) electrophoretic coating (low magnification), and d) electrophoretic coating (high magnification). In both processes, heating was carried out at  $T_h = 573$  K for  $t_h = 1.8$  ks, and in the electrophoretic deposition the coating was carried out up to  $V_c = 10$  V. Figs. 4-a and 4-b show that many tunnel-pits of etched specimens are filled with an epoxy resin used for specimen embedding, instead of SiO<sub>2</sub>. It can be seen from Figs. 4-c and 4-d that the electrophoretic deposition enables the relatively uniform coating of SiO<sub>2</sub> on the inner wall of tunnel-pits.

Figure 5 shows SEM images of the surface of Specimen-II a) before SiO<sub>2</sub> coating, b) after SiO<sub>2</sub> coating by dipping, c) after coating by electrophoretic deposition up to V<sub>c</sub> = 10 V with n = 1, and d) after coating by electrophoretic deposition up to V<sub>c</sub> = 10 V with n = 2. Specimens were heated at T<sub>h</sub> = 573 K for t<sub>h</sub> = 1.8 ks after electrophoretic and dip coating. The surface of the Specimen-II before SiO<sub>2</sub> coating (Fig. 5-a) appears very smooth, while the surface after SiO<sub>2</sub> coating (Figs. 5-b, c, and d) appears rough, due to the deposition of SiO<sub>2</sub>. Comparing Fig. 5-b with Figs. 5-c and -d strongly suggest that electrophoretic deposition results in much more uniform coating than dip process.

Table1 shows the mass gain of specimens-I and -II by dip coating and electrophoretic coating with i<sub>c</sub> = 0.05, 0.1, and 0.2 A m<sup>-2</sup>. After dip and electrophoretic deposition, the specimens were heated at T<sub>h</sub> = 573 K for t<sub>h</sub> = 1.8 ks in O<sub>2</sub>-atmosphere. The mass gain of each specimen by electrophoretic deposition is much larger than that by dip coating, suggesting the effect of electric field is significant for uniform coating of SiO<sub>2</sub>. Mass gain by electrophoretic process does not depends on current density on Specimen-I, while it slightly decreases with increasing c. d. on Specimen-II.

The amount of  $O^{2-}$  ions in anodic oxide films formed by electrophoretic coating can be estimated from Fig. 3-a to be ca.  $0.014 \text{ g m}^{-2}$ , assuming that the inner layer is composed of  $Al_2O_3$  with a density of  $3,000 \text{ kg m}^{-3}$ . This amount corresponds to only 10 % of mass gain on Specimen-I and 4 % on Specimen-II. The mass gain by electrophoretic coating on Specimen-II is much larger than that on Specimen-I, suggesting that excess sol in micro-pits of Specimen-II leads to the larger mass gain.

### 3. 2 Anodic oxide film formation on $SO_2$ -coated specimen in Solution-1

Figure 6 shows the  $E_a$  vs.  $t_a$  curves obtained in Solution-1 on a) Specimen-I and b) Specimen-II, which were coated with  $SiO_2$  layers at  $i_c = 0.05 - 0.2 \text{ Am}^{-2}$  before heat treatment at  $T_h = 573 \text{ K}$  for  $t_h = 1.8 \text{ ks}$ . The  $E_a$  vs.  $t_a$  curve for Specimens-I and -II without any coating is also indicated as broken lines. Specimen-I coated with  $SiO_2$  shows a 10 V-jump in  $E_a$  at the initial stage, and then linear increase in  $E_a$  with  $t_a$ . The slope of  $E_a$  vs.  $t_a$  curves for Specimen-1 with  $SiO_2$ -coating is slightly steeper than that without  $SiO_2$ -coating, and does not depend on  $i_c$ . The steeper slopes of the  $E_a$  vs.  $t_a$  curves on  $SiO_2$ -coated Specimen-I suggest the formation of Al-Si composite oxide films.

All the  $E_a$  vs.  $t_a$  curve on Specimen-II (Fig. 6-b) shows a slightly upwards curved line unlike on Specimen-I, and this is because the surface area of specimens decreases gradually with increasing  $E_a$  on Specimen-II, due to the filling of micro-tunnel pits with anodic oxide films. The slope of the curves on  $\text{SiO}_2$ -coated Specimen-II is steeper than that on  $\text{SiO}_2$ -coated Specimen-I and becomes steeper at lower  $i_c$ . Smaller  $i_c$  seems to allow the formation of Al-Si composite oxide films more uniformly on the inner wall of tunnel pits of Specimen-II. This can be expected from larger mass gains in electrophoretic coating at smaller  $i_c$  (see Table 1).

Figure 7 shows the effect of heating temperature,  $T_h$ , and repetition number of coating,  $n$ , on  $E_a$  vs.  $t_a$  curve on Specimen-II. Current density during electrophoretic deposition,  $i_c$ , was  $0.05 \text{ A m}^{-2}$  on all the specimens examined here, and in the case of  $n = 2$ , the procedure of  $\text{SiO}_2$  coating is the same as that shown in Fig. 6. It can be seen from Fig. 7 that  $T_h = 773 \text{ K}$  gives the steepest slope of  $E_a$  vs.  $t_a$  curves, and that the effect of  $T_h$  and  $n$  on the anodizing behavior is not significant at temperatures below  $T_h < 673 \text{ K}$ . The steepest slope with  $T_h = 773 \text{ K}$  is difficult to explain, but it can be expected that higher heating temperature causes the formation of more anhydrous  $\text{SiO}_2$ ,

leading to the enhancement of Al-Si composite oxide layer formation during anodizing.

Figure 8 shows TEM images of the vertical cross sections of Specimen-I with SiO<sub>2</sub>-coating and anodizing up to a) 100V, b) 200V and c) 300V. The SiO<sub>2</sub>-coating were carried out with  $i_c = 0.2 \text{ Am}^{-2}$  up to  $V_c = 10 \text{ V}$  before heating at  $T_h = 573 \text{ K}$  for  $t_h = 1.8 \text{ ks}$ . All the films show two layers underneath SiO<sub>2</sub> layer: an outer layer and an inner layer. EDX analysis showed that the inner layer is composed of alumina, and the outer layer is composed of Al-Si composite oxide. Both layers become thicker with  $E_a$ , while SiO<sub>2</sub> layer becomes thinner. This can be explained in terms of the conversion of SiO<sub>2</sub> to Si-Al composite oxide and the formation of Al<sub>2</sub>O<sub>3</sub><sup>17)</sup>. The sum of thicknesses of the outer and inner layers at  $E_a = 300 \text{ V}$  is ca. 330 nm, indicating 1.1 nm / V of K-value, which is much smaller than 1.5 nm / V for anodic oxide films formed on electropolished aluminum. This is due to the high electric field sustainability of Al-Si composite oxide layer.

Figure 9 shows the TEM image of the cross section of Specimen-II after electrophoretic coating and anodizing. Electrophoretic coating was carried out under the conditions of  $i_c = 0.05 \text{ Am}^{-2}$ ,  $V_c = 10 \text{ V}$ ,  $T_h = 573 \text{ K}$ , and  $t_h = 1.8 \text{ ks}$  and anodizing

was carried out up to  $E_a = 100$  V in Solution-I. There appears an anodic oxide film on the inner wall of a tunnel pit, which was cut into round slices. Agglomerated  $\text{SiO}_2$  is observed on the anodic oxide film at the inside of the tunnel pit, and its thickness is not uniform. The anodic oxide film is composed of two layers: an inner structure-less layer and an outer small particle-dispersed layer. The inner layer may be composed of  $\text{Al}_2\text{O}_3$  and the outer layer of Al-Si composite oxide.

### 3.3 Dielectric properties of anodic oxide films formed on $\text{SiO}_2$ coated specimen

Figure 10 shows the relationship between the reciprocal of parallel capacitance,  $1 / C_p$ , of anodic oxide films and anode potential,  $E_a$ , obtained for Specimen-I coated with  $\text{SiO}_2$  at  $i_c = 0.2 \text{ Am}^{-2}$  up to  $V_c = 10$  V and  $T_h = 573, 673$  and  $773$  K. Anodizing condition is as described in the experimental section ( $i_a = 10 \text{ A m}^{-2}$ ,  $T_a = 293$  K,  $0.5 \text{ kmol m}^{-3}\text{-H}_3\text{BO}_3 / 0.05 \text{ kmol m}^{-3}\text{-Na}_2\text{B}_4\text{O}_7$  (Solution-I)). The  $1 / C_p$  values of all the specimens are proportional to  $E_a$ . The  $T_c = 573$  K specimen has the same slope as the specimen without coating, while specimens with higher  $T_h$ s have flatter slopes. This indicates that anodic oxide films formed on Specimen-I with  $\text{SiO}_2$  films have higher

parallel capacitances, and that the tendency is pronounced at higher heating temperatures, showing 20 % at  $T_h = 773$  K .

The  $1 / C_p$  vs.  $E_a$  curves obtained for Specimen-II coated with  $\text{SiO}_2$  at  $i_c = 0.05$   $\text{Am}^{-2}$  and  $T_h = 573, 673$  and  $773$  K showed straight lines passing the origin, and the slope of the curves was flatter at higher  $T_h$ s. The  $C_p$  of anodic oxide films formed on Specimen-II after  $\text{SiO}_2$  coating at  $T = 773$  K was 7 % larger than that on Specimen-II without coating.

#### 3.4 Anodic oxide films formed in Solution-II after $\text{SiO}_2$ coating on Specimen-II

Anodizing of aluminum in Solution-II enables the formation of anodic oxide films with a film breakdown potential as high as  $1,000 \text{ V}^{(26-28)}$ . The authors, here, show the effect of  $\text{SiO}_2$  coating on the formation and dielectric properties of such anodic oxide films on Specimen-II. Figure 11 shows the changes in anode potential,  $E_a$ , with time,  $t_a$ , during anodizing of Specimen-II in Solution-II before / after  $\text{SiO}_2$  coating. The  $\text{SiO}_2$  coating was carried out by two-step process: the first electrophoretic deposition with  $0.2 \text{ A m}^{-2}$  up to  $20.5 \text{ V}$  before heating at  $T_h = 573$  K for  $t_h = 1.8$  ks and the second

electrophoretic deposition with  $0.2 \text{ A m}^{-2}$  up to 24.5 V before heating under the same conditions. It can be seen from Fig. 11 that  $E_a$  increases with  $t_a$  on both non-coated and  $\text{SiO}_2$ -coated specimens, and that the slope of  $E_a$  vs.  $t_a$  curves becomes flatter at  $E_a = 1050 \text{ V}$ , due to the start of film breakdown. Both curves show oscillation in potential, and the oscillation becomes more remarkable with increasing  $E_a$ , especially after film breakdown starts. Before film breakdown, the  $\text{SiO}_2$ -coated specimen shows steeper slope of the  $E_a$  vs.  $t_a$  curve than non-coated one, and smaller potential oscillation.

Figure 12 shows SEM images of the surface of Specimen-II a) before anodizing (no coating), b) before anodizing ( $\text{SiO}_2$  coating), c) after anodizing up to 1,000 V (no coating), and d) after anodizing up to 1,000 V ( $\text{SiO}_2$  coating). Specimen-II as received (Fig. 12-a) shows many pits with sharp edges, while on the specimen after  $\text{SiO}_2$  coating (Fig. 12-b) there are pits filled with  $\text{SiO}_2$  and pit edges are slightly milder than those on the specimen as received. After anodizing up to 1,000 V of Specimen-II with / without  $\text{SiO}_2$  coating (Figs. 12-c and d), most of the pits are filled with anodic oxide films, and edge pits is much milder than those on the specimen before anodizing (Figs. 12-a and - b). Comparison of Fig. 12-c with Fig. 12-d shows that the tendency of pit-filling and

pit-edge mildening is more obvious on non-coated specimen than SiO<sub>2</sub>-coated one.

This may be due to the formation of thinner anodic oxide films on SiO<sub>2</sub>-coated specimen than on no-coated specimen.

Figure 13 shows the relationship between the reciprocal of parallel capacitance,  $1 / C_p$ , with film formation potential,  $E_a$ , obtained for Specimen-II with / without SiO<sub>2</sub> coating. The  $1 / C_p$  vs.  $E_a$  curves of both specimens show the upwards curved shape with increasing  $E_a$ , unlike the straight lines in Fig. 10, where  $1 / C_p$  is proportional to  $E_a$ . This is due to the decrease in surface area by filling of tunnel pits with anodic oxide films on Specimen-II, and the tendency becomes much more remarkable as  $E_a$  rises above 500 V.

It should be emphasized here that the value of  $1 / C_p$  for SiO<sub>2</sub>-coated specimen at each  $E_a$  is smaller than that for no-coated specimen. This is because the decrease in surface area of the specimen with increasing  $E_a$  is suppressed on SiO<sub>2</sub>-coated specimen, due to the formation of thinner anodic oxide films with higher electric field sustainability. The capacitance of  $E_a = 1,000$  V anodic oxide films formed on SiO<sub>2</sub>-coated specimen is 39 % higher than that on no-coated specimen.

Conclusively, electrophoretic coating of  $\text{SiO}_2$  on DC-etched aluminum before anodizing is very effective to increase the capacitance of anodic oxide films at high voltage.

#### 4. Conclusion

Electrophoretic sol-gel coating of  $\text{SiO}_2$  was performed on DC-etched and electropolished aluminum, and then anodizing was carried out to examine the dielectric properties of anodic oxide films. The following conclusions may be drawn.

1. Electrophoretic sol-gel coating can form  $\text{SiO}_2$  films uniformly on the surface of plain and DC-etched specimens. A thin oxide layer is formed by anodic oxidation during the formation of  $\text{SiO}_2$  film.

2. Anodizing of aluminum coated with  $\text{SiO}_2$  films leads to the formation of oxide films, which consist of an outer Al-Si composite oxide layer and an inner  $\text{Al}_2\text{O}_3$  layer underneath  $\text{SiO}_2$  layer. The anodic oxide films formed thus has a high electric field sustainability.

3. The anodic oxide films formed on specimens with  $\text{SiO}_2$  film in a boric acid /

borate solution have at most 10% higher parallel capacitance than those without SiO<sub>2</sub> layer. Higher heating temperatures after electrophoretic deposition lead to the increase in capacitance of anodic oxide films.

4. The parallel capacitance of anodic oxide films formed in a boric acid solution on DC-etched specimens with SiO<sub>2</sub> film is 39 % higher at  $E_a = 1,000$  V than that on electropolished specimens, due to the suppression of decrease in the surface area by forming thinner anodic oxide films with a higher electric field sustainability.

## 5. References

[1] H. Takahashi, Y. Umehara, T. Miyamoto, N. Fujimoto, and M. Nagayama: *J. Metal Fin. Soc. Jpn.*, **38**, 67 - 73 (1987)

[2] H. Takahashi, Y. Umehara, and M. Nagayama: *J. Metal Fin. Soc. Jpn.*, **38**, 139 - 142 (1987)

[3] H. Takahashi, Y. Umehara, R. Furuichi, and M. Nagayama: *J. Metal Fin. Soc. Jpn.*, **40**, 590 - 597 (1989)

[4] H. Takahashi, K. Takahashi, R. Furuichi, and M. Nagayama: *J. Metal Fin. Soc. Jpn.*,

**40**, 1415 - 1421 (1989)

[5] H. Takahashi, C. Ikegami, M. Seo, and R. Furuichi: *J. Electron Microsc.*, **40**, 101-109 (1991)

[6] H. Takahashi, M. Dairaku, and M. Seo: *J. Surf. Fin. Soc. Jpn.*, **45**, 810-817 (1994)

[7] M. Shikanai, M. Sakairi, H. Takahashi, M. Seo, K. Takahiro, S. Nagata, and S. Yamaguchi: *J. Electrochem. Soc.*, **144**, 2756 - 2766 (1997)

[8] H. Takahashi, H. Kamada, M. Sakairi, K. Takahiro, S. Nagata, and S. Yamaguchi: Proc. Intern. Symp. of Dielectric Material Integration for Micro Electronics, sponsored by Electrochem. Soc., p.253 -262 (1998)

[9] H.-Y. Tian and W.-G. Luo, *Mater. Chem. Phys.*, **69**, 166 – 171 (2001)

[10] M. Nayak, S. Y. Lee, and T.-Y. Tseng, *Mater. Chem. Phys.*, **77**, 34 – 42 (2002)

[11] S. U. Adikary and H. L. W. Chan, *Thin Solid Films*, **424**, 70 – 74 (2003)

[12] Y. Xu, *Ceramics Intern.*, **30**, 1741 – 1743 (2004)

[13] S.-S. Park and B.-T. Lee, *J. Electroceramics*, **13**, 111 – 116 (2004)

[14] K. Watanabe, M. Sakairi, H. Takahashi, S. Hirai, and S. Yamaguchi: *J. Surf. Fin. Soc. Jpn.*, **50** 359 -366 (1999)

- [15] K. Watanabe, M. Sakairi, H. Takahashi, S. Hirai and S. Yamaguchi; *J. Electroanal. Chem.*, **473**, 250 -255 (1999)
- [16] K. Watanabe, M. Sakairi, H. Takahashi, K. Takahiro, S. Nagata, and S. Hirai; *Electrochemistry*, **67**,1243 - 1248 (1999)
- [17] K. Watanabe, M. Sakairi, H. Takahashi, K. Takahiro, S. Nagata, and S. Hirai; *Electrochemistry*, **69**, 407 – 413 (2001)
- [18] K. Watanabe, M. Sakairi, H. Takahashi, K. Takahiro, S. Nagata, and S.Hirai; *J. Electrochem. Soc.*, **148**, B473 - 481 (2001)
- [19] K. Watanabe, M. Sakairi, H. Takahashi, and S. Hirai; *Materia*, **42**, 911 (2003)
- [20] H. Takahashi, M. Sakairi, K. Watanabe, T. Kikuchi, and M. Yamada; *J. Surf. Fin. Soc. Jpn.*, **54** [7], 436 – 441 (2003)
- [21] K. Watanabe, M. Sakairi, H. Takahashi, and S. Hirai; *J. Surf. Fin. Soc. Jpn.*, **54** [3], 235 – 240 (2003)
- [22] K. Watanabe, M. Sakairi, H. Takahashi, S. Nagata, and s. Hirai, *J. Surf. Fin. Soc. Jpn.*; **55**, 471 – 477 (2004)
- [23] K. Hasegawa, M. Tatsumisago, and T. Inami: *J. Ceramic Soc. Jpn.*, **105**, 569 (1997)
- [24] S. Sakka ; “Science of sol-gel method”, p.8 (Agne-shouhusha, 1996)

[25] R. F. Zhang, J. Ma, and L. B. Kong, *J. Mater. Research*, **17**, 933 – 935 (2002)

[26] Y. Li, H. Shimada, M. Sakairi, K. Shigyo, H. Takahashi, and M. Seo: *J. Electrochem. Soc.*, **144**, 866 - 876 (1997)

[27] H. Shimada, M. Sakairi, and H. Takahashi, *J. Surf. Fin. Soc. Jpn.* **53**, 134 - 141 (2002)

[28] H. Shimada, M. Sakairi, and H. Takahashi, *J. Surf. Fin. Soc.*, **53**, 142 - 148 (2002)

]

## Captions

Table.1 Mass gain of specimen-I and specimen-II during dip-coating and electrophoretic coating up to 10 V

Fig. 1 Time-variations in cell voltage,  $V_c$ , during electrophoretic deposition of  $\text{SiO}_2$  with different current densities of  $i_c = 0.01 - 0.2 \text{ A m}^{-2}$  on a) Specimen-I and b) Specimen-II

Fig. 2 Change in cell voltage,  $V_c$ , with time,  $t_c$ , during the second electrophoretic sol-gel coating, obtained for specimen-I. In the first step,  $\text{SiO}_2$  gel was deposited with  $i_c = 0.2 \text{ A m}^{-2}$  up to  $E_c = 5 \text{ V}$ , and then heat treatment was carried out at  $T_h = 573, 673,$  and  $773 \text{ K}$  for  $t_h = 1.8 \text{ ks}$ .

Fig. 3 TEM images of the cross section of Specimen-I after electrophoretic deposition up to  $V_c = 10 \text{ V}$  by a) one step and b) two steps. Both specimens were heated at  $T_h = 573 \text{ K}$  for  $t_h = 1.8 \text{ ks}$  after each deposition step.

Fig. 4 TEM images of the cross sections of Specimen-II after a) dip coating (low magnification), b) dip coating (high magnification), c) electrophoretic coating (low magnification), and d) electrophoretic deposition (high magnification). In both processes, heating was carried out at  $T_h = 573 \text{ K}$  for  $t_h = 1.8 \text{ ks}$ , and in the electrophoretic deposition the coating was carried out up to  $V_c = 10 \text{ V}$ .

Fig. 5 SEM images of the surface of Specimen-II a) before SiO<sub>2</sub> coating, b) after SiO<sub>2</sub> coating by dipping process, c) after coating by electrophoretic deposition up to V<sub>c</sub> = 10 V with n = 1, and d) after coating by electrophoretic deposition up to V<sub>c</sub> = 10 V with n = 2. Specimens were heated at T<sub>h</sub> = 573 K for t<sub>h</sub> = 1.8 ks after electrophoretic and dip coating.

Fig. 6 Time-variations in anode potential, E<sub>a</sub>, during anodizing in Solution-I before / after SiO<sub>2</sub> coating, obtained for a) Specimen-I and b) Specimen-II. The SiO<sub>2</sub> coating was carried out at i<sub>c</sub> = 0.05, 0.1 and 0.2. Am<sup>-2</sup> before heat treatment at T<sub>h</sub> = 573 K for t<sub>h</sub> = 1.8 ks.

Fig. 7 Effect of heating temperature, T<sub>h</sub>, and repetition number of coating, n, on E<sub>a</sub> vs. t<sub>a</sub> curve on Specimen-II. Electrophoretic deposition was carried out with i<sub>c</sub> = 0.05 A m<sup>-2</sup> up to 10 V.

Fig. 8 TEM images of the vertical cross sections of Specimen-I after SiO<sub>2</sub>-coating and anodizing up to a) 100V, b) 200V and c) 300V. The SiO<sub>2</sub>-coating were carried out with i<sub>c</sub> = 0.2 Am<sup>-2</sup> up to V<sub>c</sub> = 10 V before heating at T<sub>h</sub> = 573 K for t<sub>h</sub> = 1.8 ks.

Fig. 9 TEM image of the cross section of Specimen-II after electrophoretic coating and

anodizing. Electrophoretic coating was carried out under the conditions of  $i_c = 0.05$   $\text{Am}^{-2}$ ,  $V_c = 10$  V,  $T_h = 573$  K, and  $t_h = 1.8$  ks and anodizing was carried out up to  $E_a = 100$  V in Solution-I.

Fig. 10 Relationship between the reciprocal of parallel capacitance,  $1 / C_p$ , of anodic oxide films and anode potential,  $E_a$ , obtained for Specimen-I coated with  $\text{SiO}_2$  at  $i_c = 0.2$   $\text{Am}^{-2}$  up to  $V_c = 10$  V and  $T_h = 573, 673$  and  $773$  K.

Fig. 11 Changes in anode potential,  $E_a$ , with time,  $t_a$ , during anodizing of Specimen-II in Solution-II before / after  $\text{SiO}_2$  coating. The  $\text{SiO}_2$  coating was carried out by two-step process: the first electrophoretic deposition with  $0.2$   $\text{A m}^{-2}$  up to  $20.5$  V before heating at  $T_h = 573$  K for  $t_h = 1.8$  ks and the second electrophoretic deposition with  $0.2$   $\text{A m}^{-2}$  up to  $24.5$  V before heating under the same conditions.

Fig. 12 SEM images of the surface of Specimen-II a) as received b) after  $\text{SiO}_2$  coating, c) after anodizing up to  $1,000$  V without any coating and d) after  $\text{SiO}_2$  coating and anodizing up to  $1,000$  V

Fig.13 Relationship between the reciprocal of parallel capacitance,  $1 / C_p$ , with film formation potential,  $E_a$ , obtained for Specimen-II with / without  $\text{SiO}_2$  coating.

Table.1 Mass gain of specimen-I and specimen-II during dipping and electrophoretic coating up to 10 V

Specimen	Mass gain $\text{g m}^{-2}$			
	Dipping $t = 1.8 \text{ ks}$	Electrophoretic		
		$i_c = 0.05 \text{ A m}^{-2}$	$i_c = 0.1 \text{ A m}^{-2}$	$i_c = 0.2 \text{ A m}^{-2}$
I	0.03	0.15	0.13	0.15
II	0.05	0.36	0.35	0.31

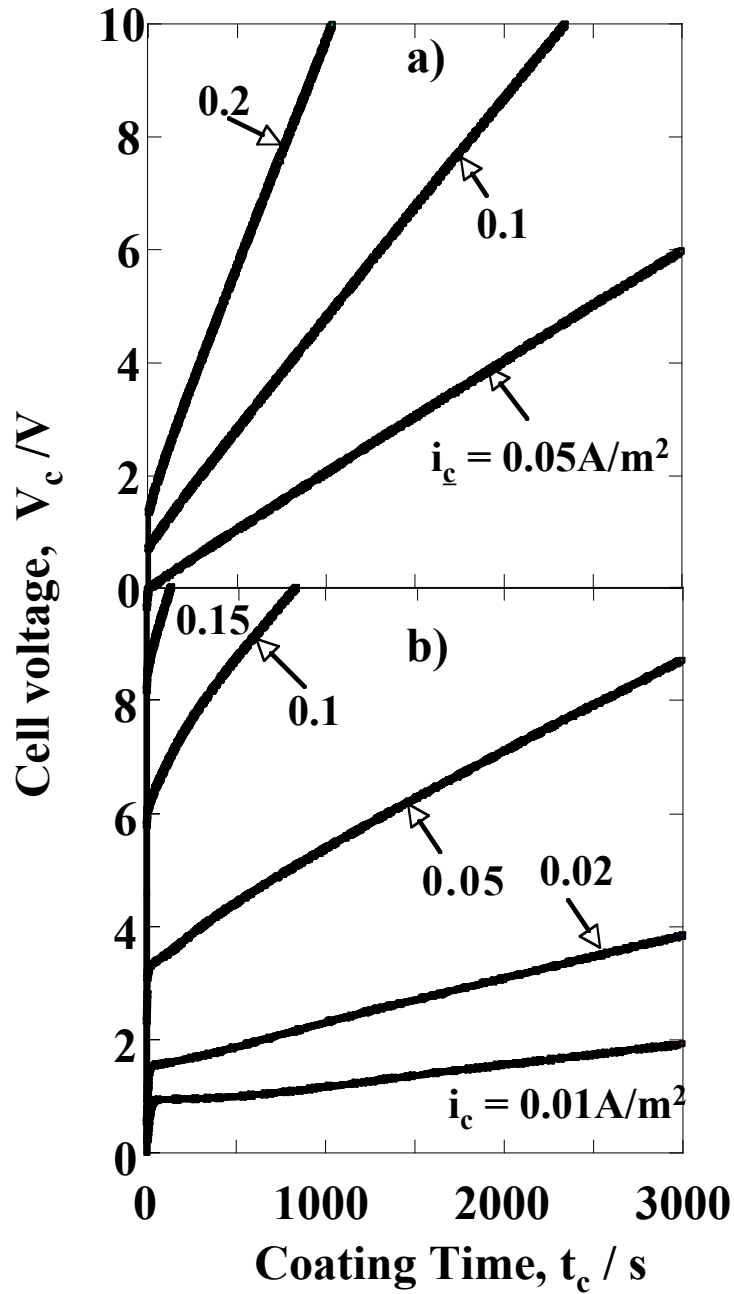


Fig. 1 Time-variations in cell voltage,  $V_c$ , during electrophoretic deposition of  $SiO_2$  with different current densities of  $i_c = 0.01 - 0.2 A m^{-2}$  on a) Specimen-I and b) Specimen-II .

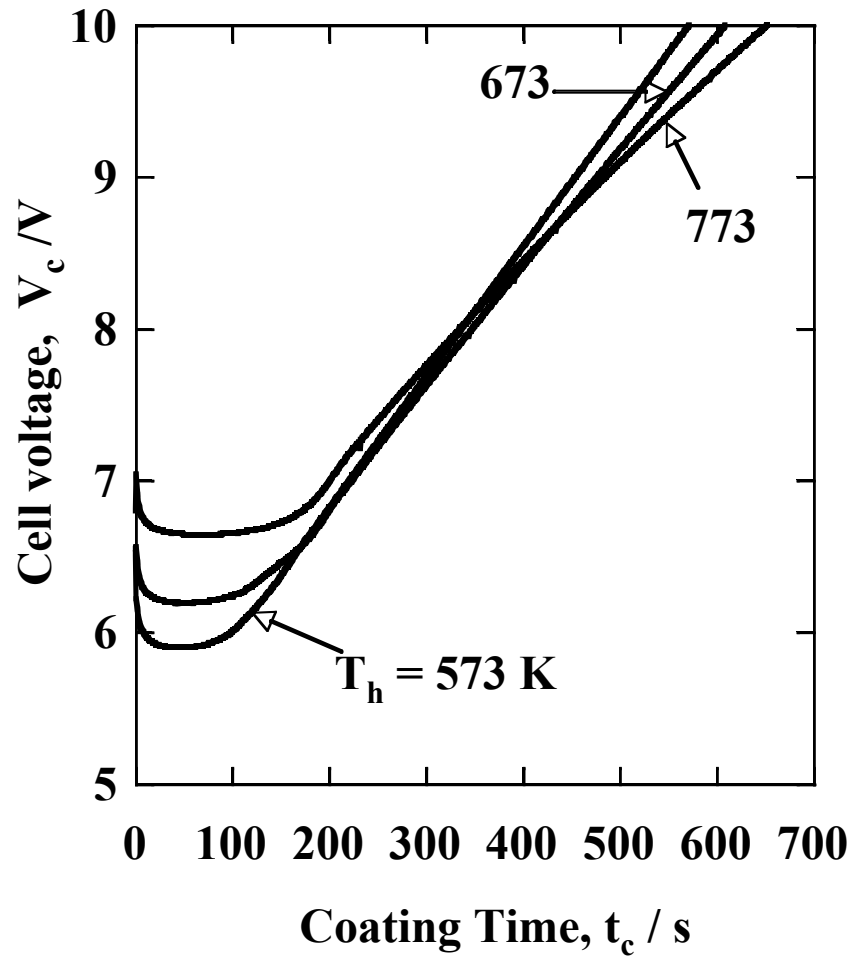


Fig. 2 Change in cell voltage,  $V_c$ , with time,  $t_c$ , during the second electrophoretic sol-gel coating, obtained for specimen-I. In the first step,  $\text{SiO}_2$  gel was deposited with  $i_c = 0.2 \text{ A m}^{-2}$  up to  $E_c = 5 \text{ V}$ , and then heat treatment was carried out at  $T_h = 573, 673, \text{ and } 773 \text{ K}$  for  $t_h = 1.8 \text{ ks}$ .

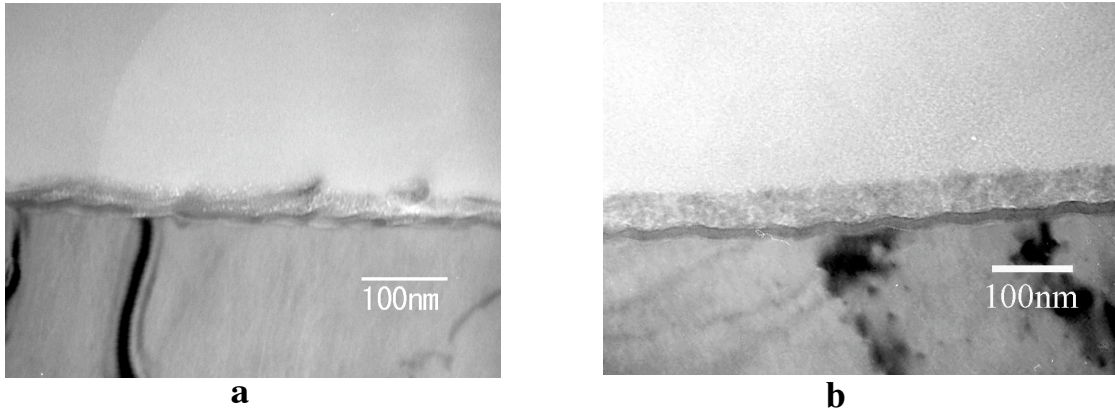


Fig. 3 TEM images of the cross section of Specimen-I after electrophoretic deposition up to  $V_c = 10$  V by a) one step and b) two steps. Both specimens were heated at  $T_h = 573$  K for  $t_h = 1.8$  ks after each deposition step.

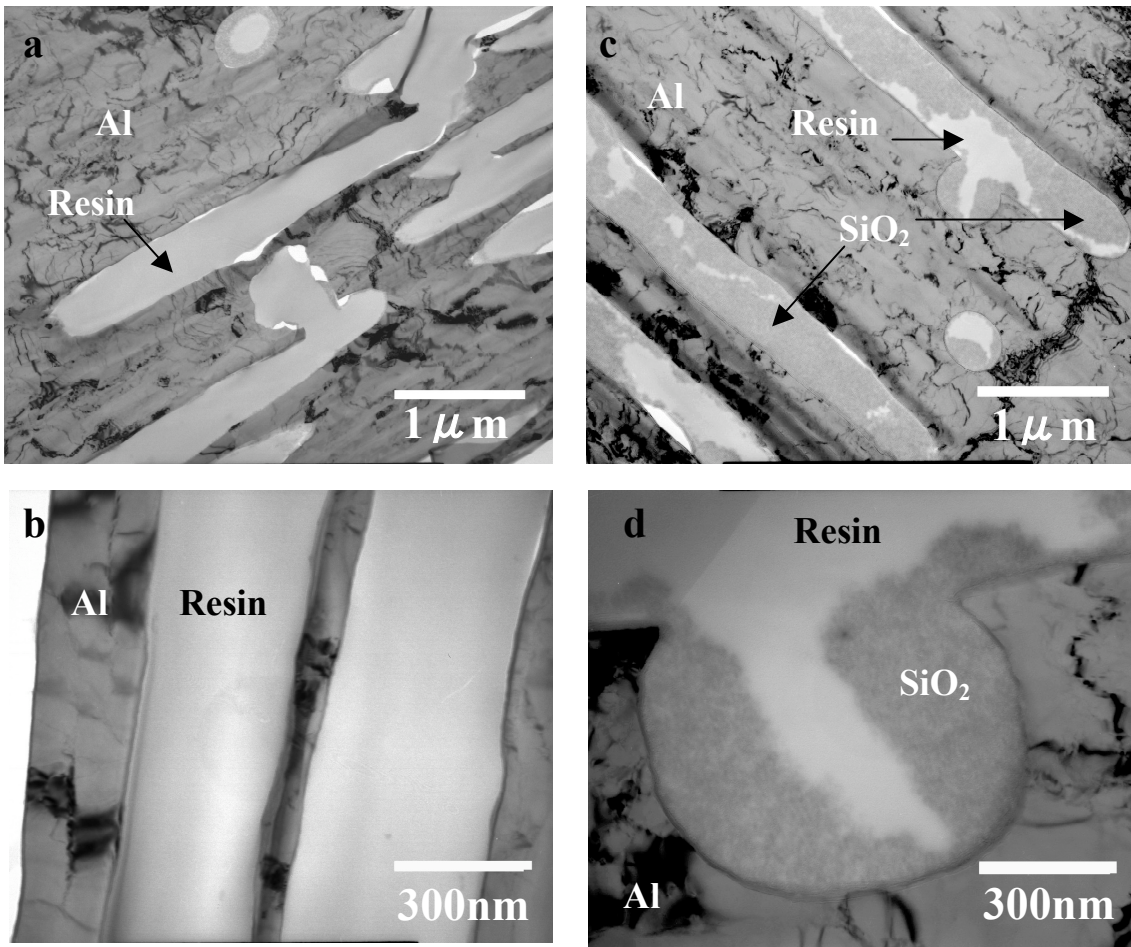


Fig. 4 TEM images of the cross sections of Specimen-II after a) dip coating (low magnification), b) dip coating (high magnification), c) electrophoretic coating (low magnification), and d) electrophoretic deposition (high magnification). In both processes, heating was carried out at  $T_h = 573 \text{ K}$  for  $t_h = 1.8 \text{ ks}$ , and in the electrophoretic deposition the coating was carried out up to  $V_c = 10 \text{ V}$ .

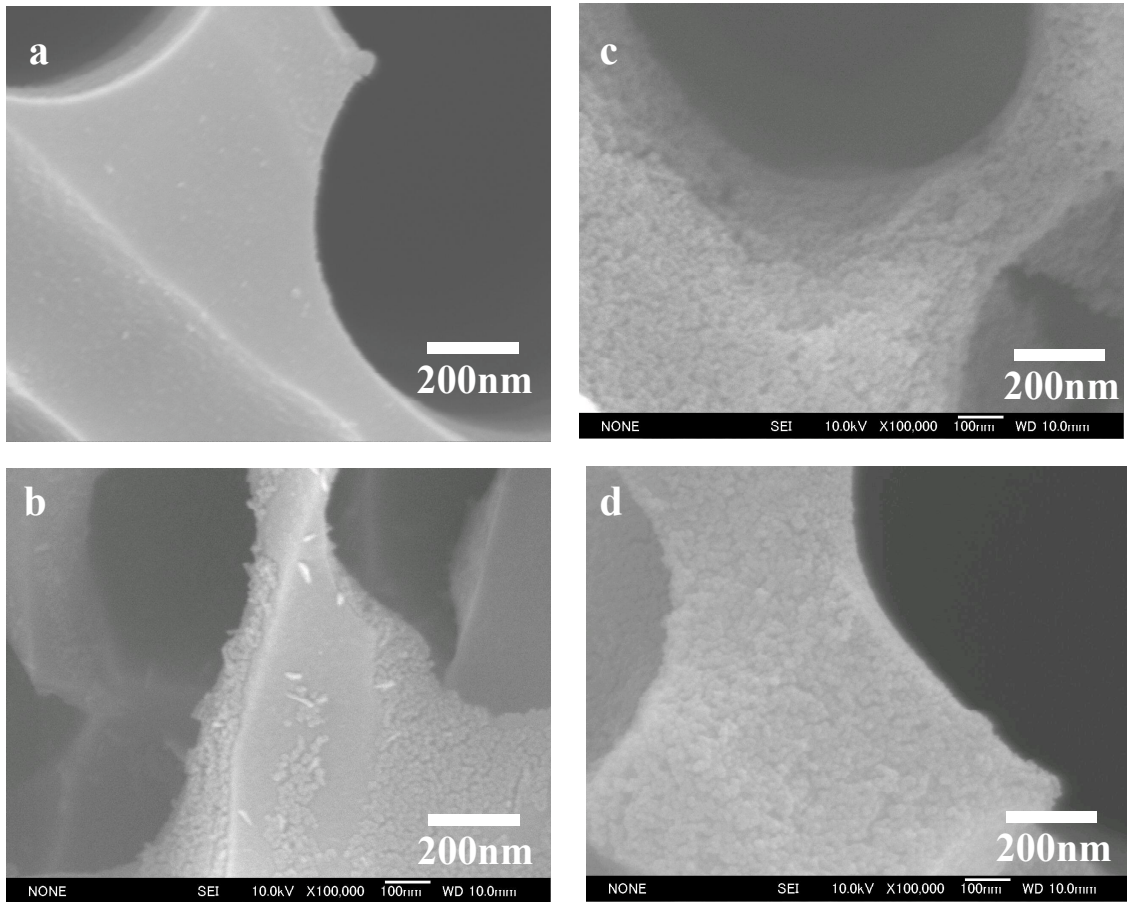


Fig. 5 SEM images of the surface of Specimen-II a) before  $\text{SiO}_2$  coating, b) after  $\text{SiO}_2$  coating by dipping process, c) after coating by electrophoretic deposition up to  $V_c = 10$  V with  $n = 1$ , and d) after coating by electrophoretic deposition up to  $V_c = 10$  V with  $n = 2$ . Specimens were heated at  $T_h = 573$  K for  $t_h = 1.8$  ks after electrophoretic and dip coating.

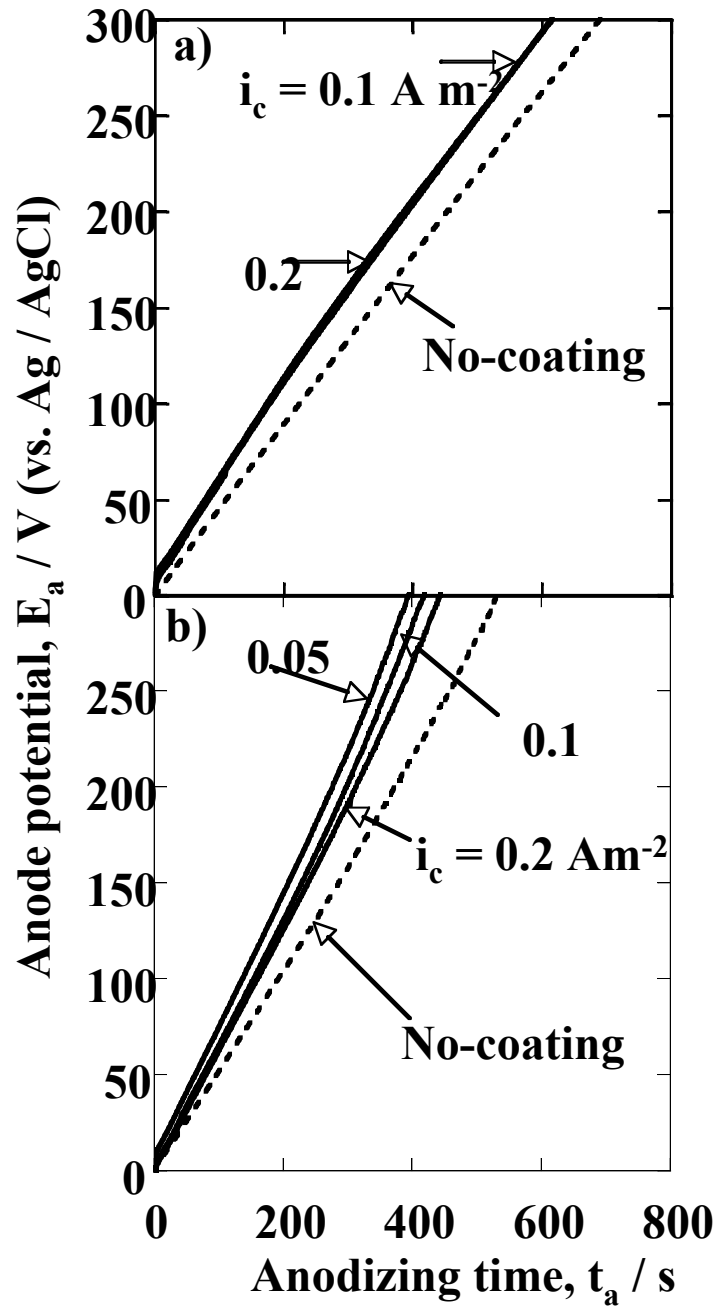


Fig. 6 Time-variations in anode potential,  $E_a$ , during anodizing in Solution-I before / after  $\text{SiO}_2$  coating, obtained for a) Specimen-I and b) Specimen-II. The  $\text{SiO}_2$  coating was carried out at  $i_c = 0.05, 0.1$  and  $0.2 \text{ Am}^{-2}$  before heat treatment at  $T_h = 573 \text{ K}$  for  $t_h = 1.8 \text{ ks}$ .

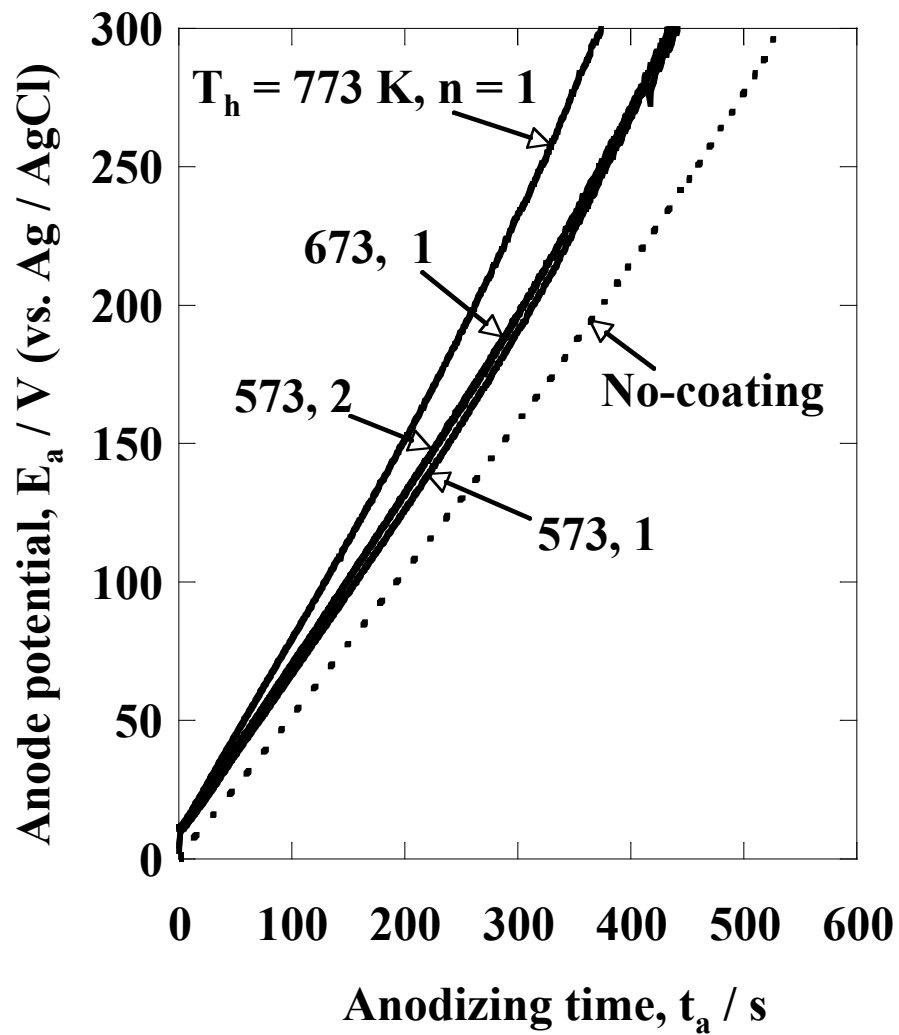


Fig. 9 Effect of heating temperature,  $T_h$ , and repetition number of coating,  $n$ , on  $E_a$  vs.  $t_a$  curve on Specimen-II. Electrophoretic deposition was carried out with  $i_c = 0.05 \text{ A m}^{-2}$  up to 10 V.

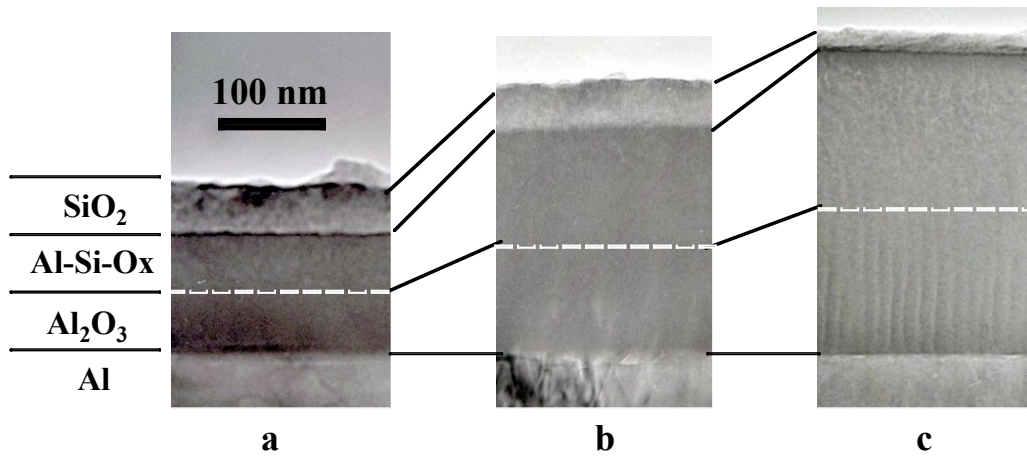


Fig. 8 TEM images of the vertical cross sections of Specimen-I after SiO<sub>2</sub>-coating and anodizing up to a) 100V, b) 200V and c) 300V. The SiO<sub>2</sub>-coating were carried out with  $i_c = 0.2 \text{ Am}^{-2}$  up to  $V_c = 10 \text{ V}$  before heating at  $T_h = 573 \text{ K}$  for  $t_h = 1.8 \text{ ks}$ .

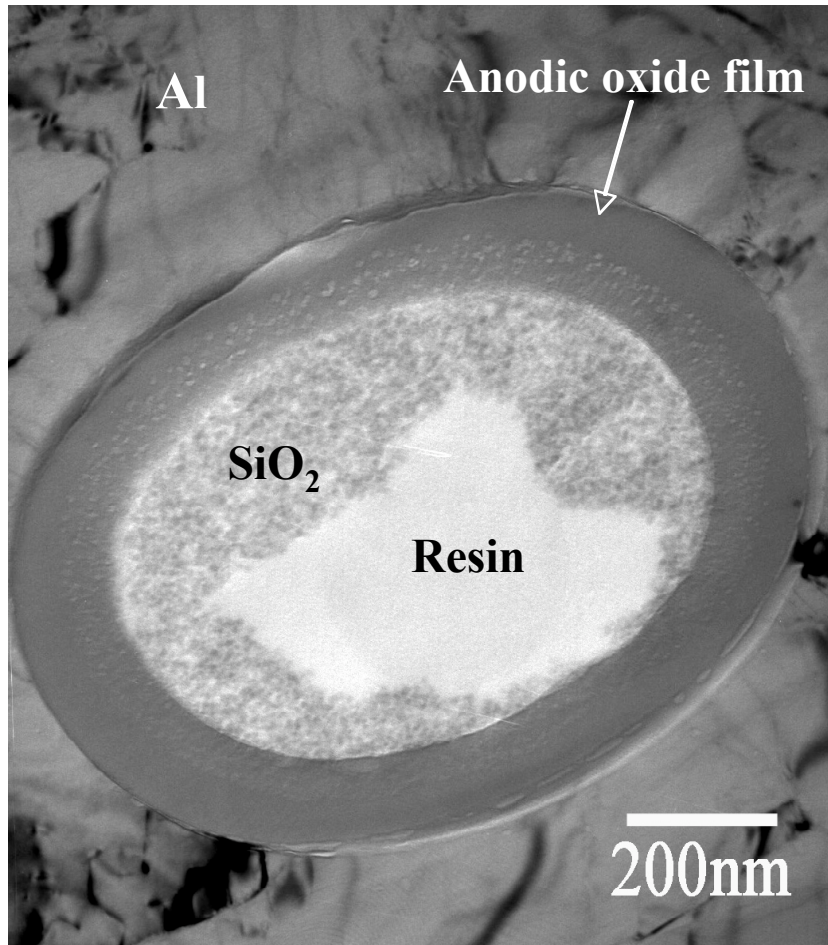


Fig. 9 TEM image of the cross section of Specimen-II after electrophoretic coating and anodizing. Electrophoretic coating was carried out under the conditions of  $i_c = 0.05 \text{ Am}^{-2}$ ,  $V_c = 10 \text{ V}$ ,  $T_h = 573 \text{ K}$ , and  $t_h = 1.8 \text{ ks}$  and anodizing was carried out up to  $E_a = 100 \text{ V}$  in Solution-I.

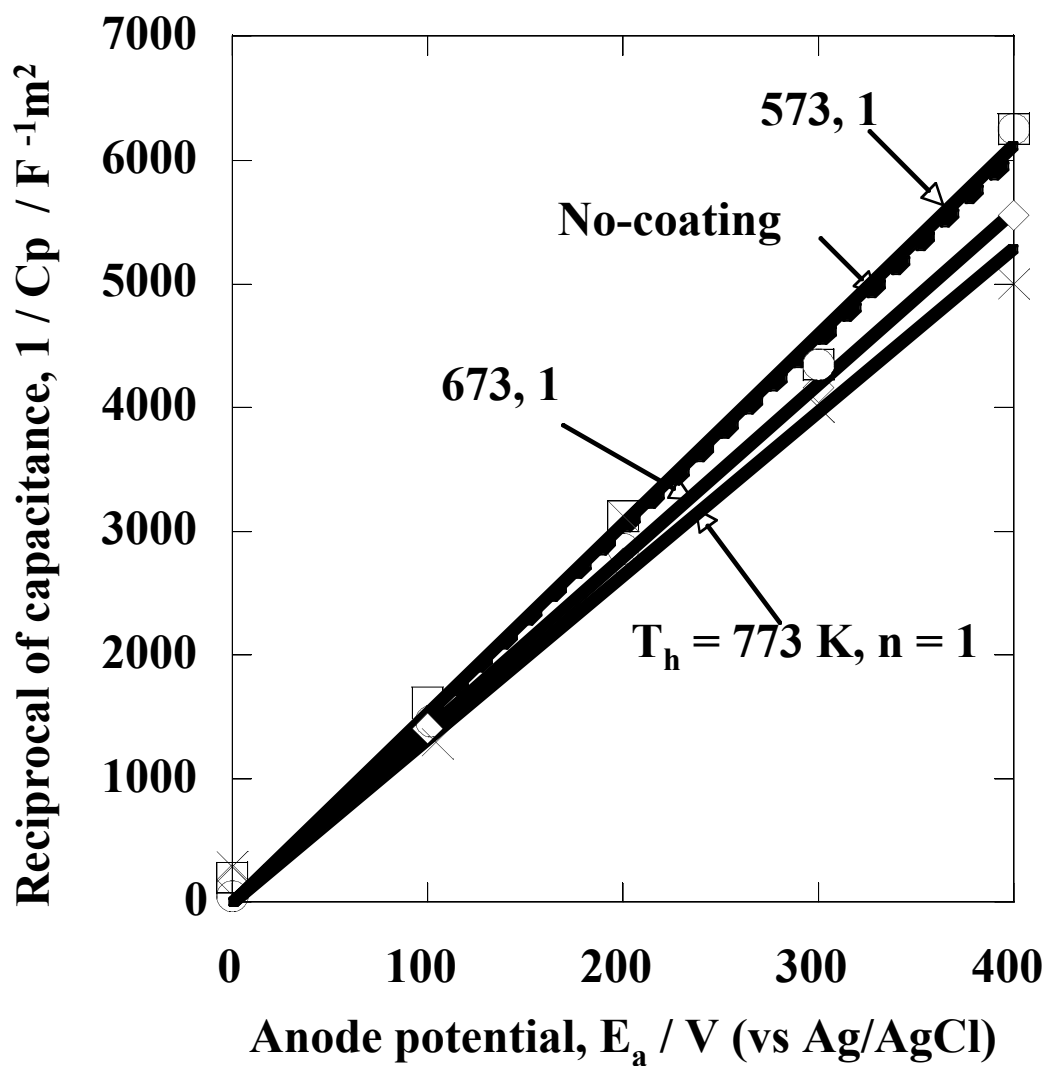


Fig. 10 Relationship between the reciprocal of parallel capacitance,  $1 / C_p$ , of anodic oxide films and anode potential,  $E_a$ , obtained for Specimen-I coated with  $SiO_2$  at  $i_c = 0.2 \text{ Am}^{-2}$  up to  $V_c = 10 \text{ V}$  and  $T_h = 573, 673$  and  $773 \text{ K}$ .

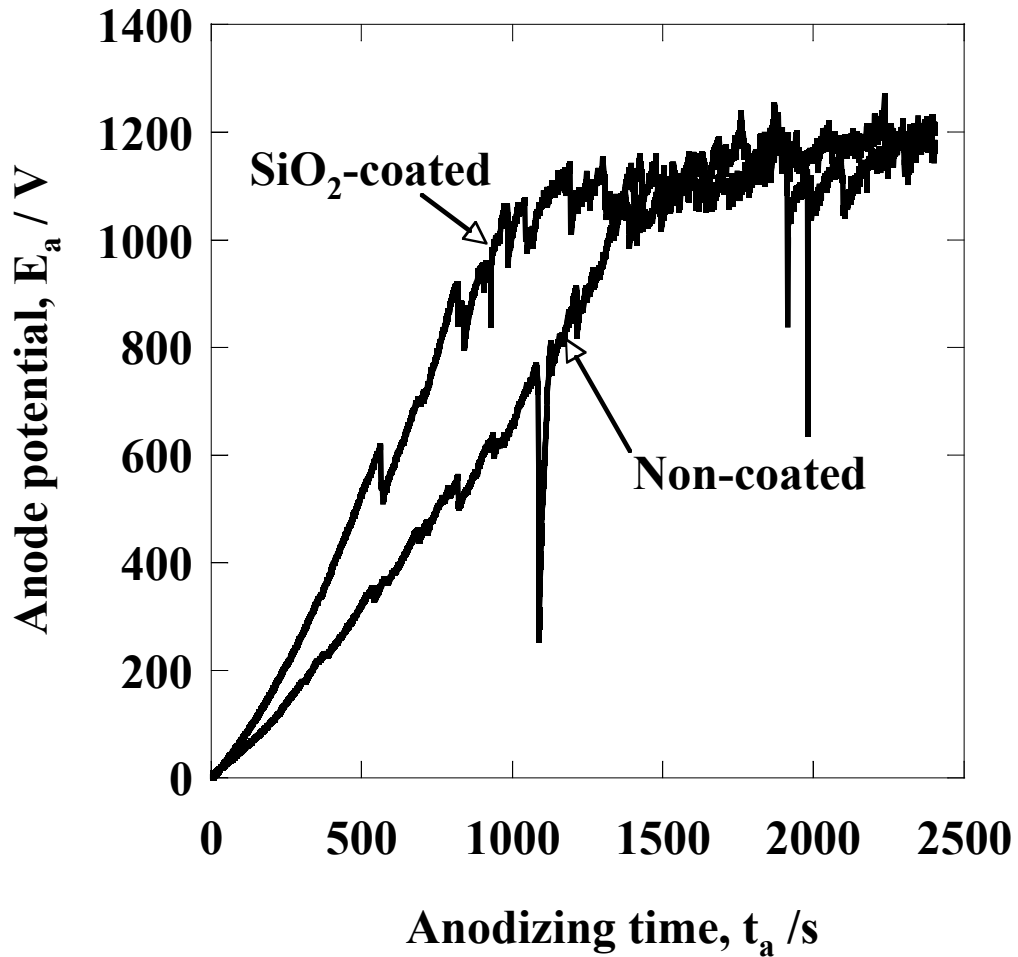


Fig. 11 Changes in anode potential,  $E_a$ , with time,  $t_a$ , during anodizing of Specimen-II in Solution-II before / after SiO<sub>2</sub> coating. The SiO<sub>2</sub> coating was carried out by two-step process: the first electrophoretic deposition with  $0.2 \text{ A m}^{-2}$  up to 20.5 V before heating at  $T_h = 573 \text{ K}$  for  $t_h = 1.8 \text{ ks}$  and the second electrophoretic deposition with  $0.2 \text{ A m}^{-2}$  up to 24.5 V before heating under the same conditions.

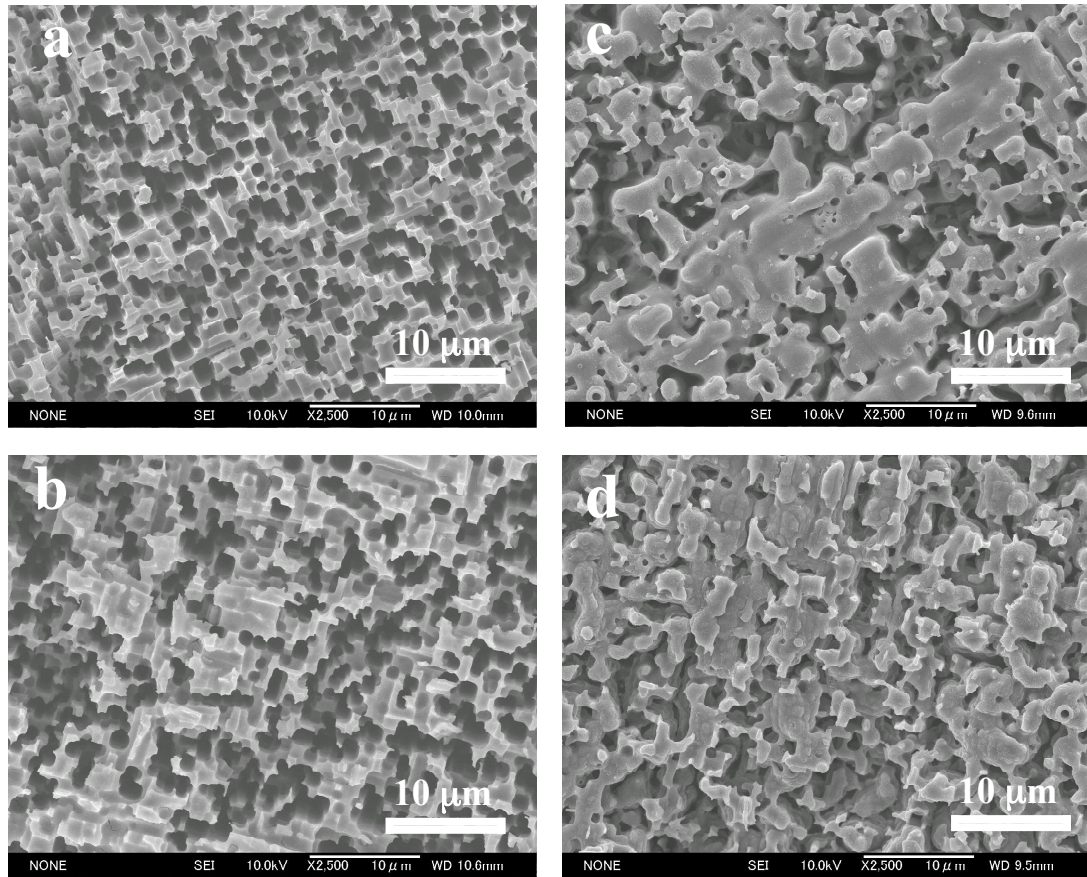


Fig. 12 SEM images of the surface of Specimen-II a) as received b) after  $\text{SiO}_2$  coating, c) after anodizing up to 1,000 V without any coating and d) after  $\text{SiO}_2$  coating and anodizing up to 1,000 V

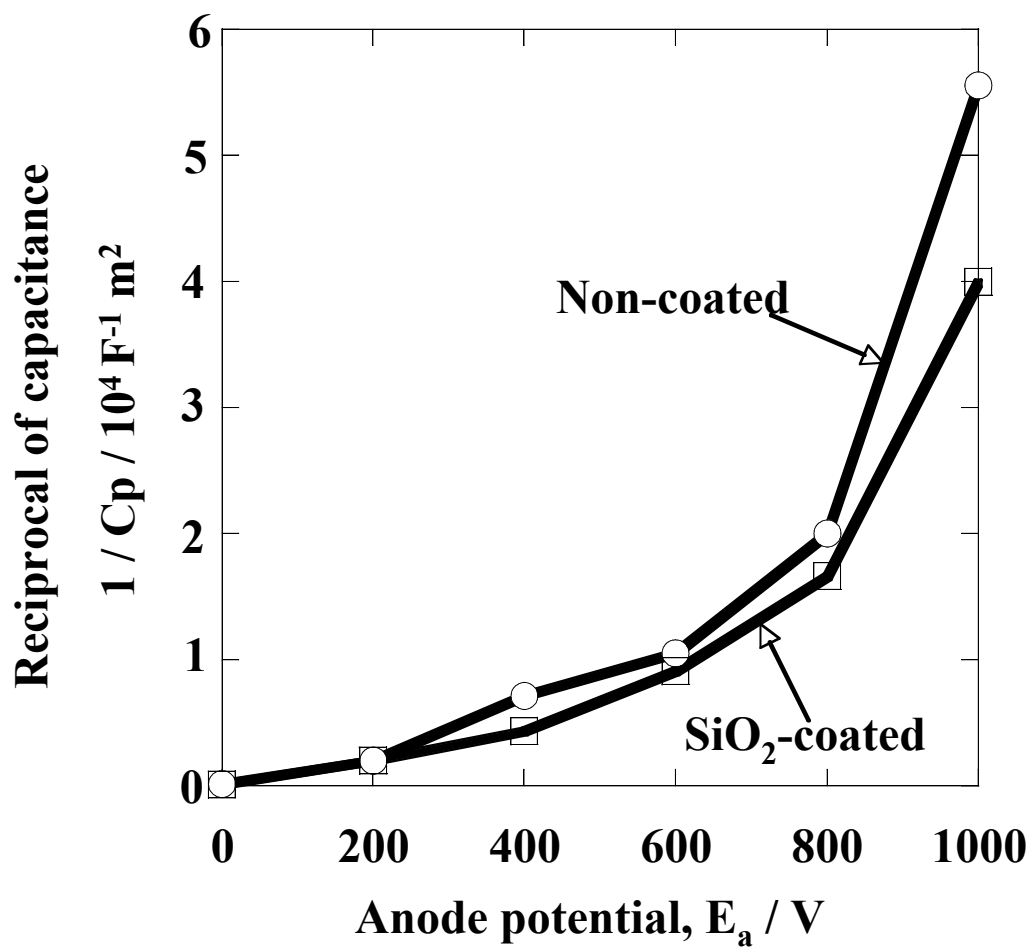


Fig.13 Relationship between the reciprocal of parallel capacitance,  $1 / C_p$ , with film formation potential,  $E_a$ , obtained for Specimen-II with / without  $\text{SiO}_2$  coating.